NASTRAN ANALYSIS OF HEAT-TRANSFER FLUID FILL PIPE FAILURES

J. Ronald Winter
Tennessee Eastman Company

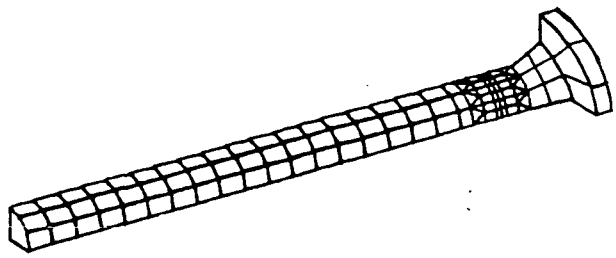

SUMMARY

Failure analysis can be a very demanding endeavor that requires a great deal of interdisciplinary assistance if the correct solution to a particular problem is to be found. This paper presents an example that shows the difficulties one can encounter in such analyses and the advantage of the finite element method (NASTRAN) in assisting one in determining the true cause of a failure. In this example, cracks were developing along a pipe weld. After discarding several possible causes for the failures, it was finally determined that the problem was due to stress-corrosion-cracking associated with a rather unusual and novel environmental condition.

INTRODUCTION

In performing failure analysis an engineer often investigates numerous possible causes of a failure before he finally determines the real reason or reasons for the particular failure. This is usually due to either the lack of sufficient information or incorrect information. In many cases he must also either prove or disprove the reasons for the failure put forth by others. This situation is especially true in domestic industry and to a somewhat lesser extent in non-domestic establishments. In this paper, all of these important facts are presented rather than just the final solution. This should help new engineers in developing the logic for attacking such problems, and to be aware of the pitfalls and other oddities with which one must contend in order to obtain a successful solution. Hopefully, it will also make new engineers more aware of the need for assistance from other fields of engineering. Such interdisciplinary assistance is often a necessity for solving certain problems.

BACKGROUND

At the time this particular problem was presented to the author, five previous failures had been encountered. The failures consisted of cracks in the fill pipe (stand pipe) of a closed (noncirculating) Dowtherm* (heat-transfer

*Trademark of Dow Chemical Company.

fluid) system used to maintain the temperature of several spin blocks in a polyester spinning plant. The basic layout of the assembly which is relevant to this presentation is shown in Figure 1. The fill pipe and the location of the failure are shown in Figure 2. Detailed dimensions of the fill pipe are shown in Figure 3. The initial five failures consisted of cracks that mimicked bending fatigue failures. This had led several persons to believe that the failures were due to vibration induced by surrounding equipment or from some large vibrating dryers at another location in the building. These particular dryers had previously produced severe structural oscillations during transient conditions (start-up, shutdown, and coast down). This was the basic situation that existed when the author started the investigation.

The need for an accurate solution to this problem increased dramatically as the number and frequency of failures increased due to the associated increase in lost production and the fire hazard associated with heat-transfer fluid leaks. Several minor fires were encountered before the problem was corrected.

INITIAL ANALYSIS

Although the failures did have the appearance of bending fatigue, I doubted this explanation because of the relatively large stiffness of the fill pipe assembly and the fact that any large oscillations that had been encountered were in the Z direction (axial to the pipe) rather than in the X or Y (lateral) directions necessary to cause bending fatigue failures. But this remained to be proven.

Since I was working on numerous other jobs at this time, the easiest and fastest way to perform the required vibration analysis was undertaken. This involved using a very simple NASTRAN finite element model* of the fill pipe. Using this method allowed me to easily account for the gusset stiffness and the tapered section of the flange. First, a normal mode (real eigenvalue) analysis was performed. This showed that the first natural frequency of this system was approximately 65 cps which, as expected, was far beyond the operating frequency of any of the vibrating equipment or electrical motors. The same model was then used to perform a forced response analysis using the transient oscillations associated with the vibrating dryers as the forcing function. See Figure 4 for a typical response plot. This further indicated that vibration was not the problem. A frequency response analysis was also performed via NASTRAN which indicated the same results. With this data in hand, it was then concluded that the failures were not associated with vibration. This fact was forwarded to the production and maintenance personnel along with a request to save the next failure for careful inspection of the failure surfaces. All previous failures had been repaired by either cutting out the cracked region and rewelding or by installing a new section of pipe.

*The model consisted of BAR elements for the pipe, plate elements for the gussets and a CØNM element for the heavy flange. See Figure 3.

Within a few weeks, two additional failures were encountered. One occurred on a new assembly and one was a repeat failure. The repeat failure had been in service about three months. Most of the previous failures had been encountered in three to six month intervals. But there were several assemblies that had not failed even though they had been in operation for over a year. Thus, it became evident that a considerable amount of information was missing.

As requested, the last two failures were held for me. They were taken to the materials laboratory where a micro-hardness test was performed. The micro-hardness test results indicated a substantial decrease in ductility in the weld region near the cracks. Due to an unusually heavy materials lab work load, no further metallurgical examinations were performed at this time.

From the preparation of the initial NASTRAN model, I had become quite aware of the different materials of construction; i.e., stainless steel and carbon steel. The difference in the coefficients of thermal expansion for these materials would result in a differential thermal dilation (radial expansion) in the weld region. Such a situation results in the development of discontinuity stresses. Such discontinuity stress might at least partially explain the large hardness variations in the axial direction at the weld. Of course, some hardness variations were expected due to the residual stresses associated with welding. However, the variations were greater than anticipated.

To evaluate the discontinuity stresses in the material transition region, I decided to apply the theory of beams on elastic foundations to this problem.[1,2] Two cases were employed in an attempt to bound the cause of the failures; i.e., one situation with conservative boundary conditions and the other with nonconservative boundary conditions. The first case consisted of assuming that the carbon section (flange) was infinitely stiff relative to the stainless steel pipe. These boundary conditions are shown below. The applicable equations are shown in Appendix A, Case A.

CONSERVATIVE CASE

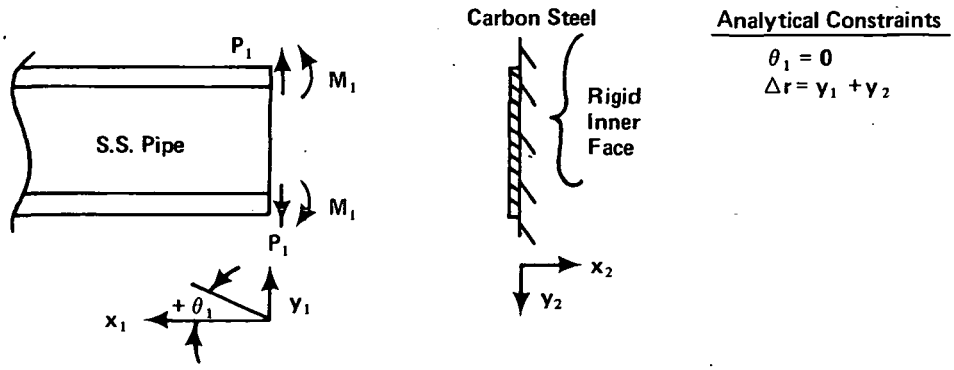

These relationships predicted stress levels far beyond the yield point of the material [>206.85 MPa (30,000 psi)]. Since there was no evidence of such exceedingly high stress levels, this result was discarded.

The second and hopefully nonconservative boundary conditions consisted of treating the weld region as the juncture of two infinitely long pieces of pipe, one made of stainless steel, the other of carbon steel. The boundary conditions for this situation are shown below. The applicable equations are presented in Appendix A, Case B.

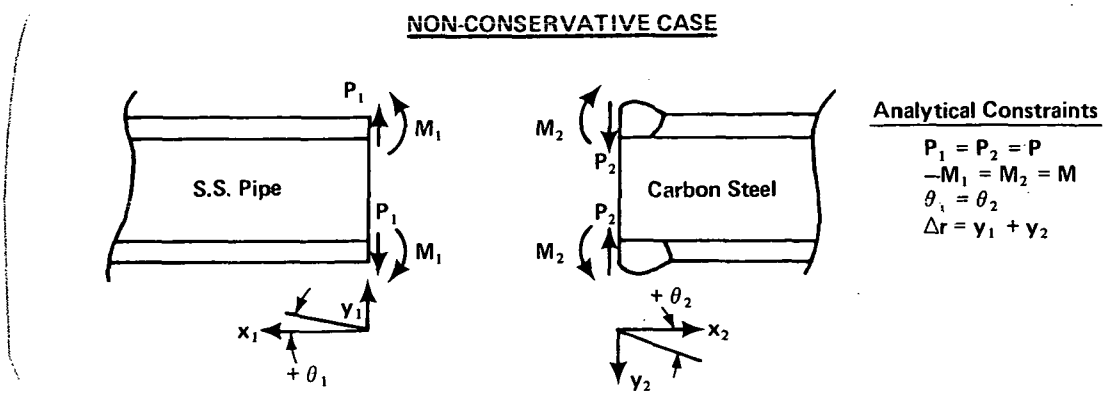

This analytical condition also predicted stress levels well beyond yield. From past experience, I knew that stress levels of this magnitude would produce local deformation that one could easily feel and in most cases could be seen by the naked eye. However, a careful inspection of the samples did not reveal the evidence necessary to support these conditions.

From this dilemma came the realization that the assumption of an abrupt change in material properties at the weld was actually incorrect. Proper treatment of the material properties along the fill pipe especially in the weld region should yield a more reasonable answer. This would, however, be a relatively time consuming, if not impossible, task to employ using the theory of beams on elastic foundations. But the finite element method would allow one to easily simulate materials variations and thus obtain reasonably good results even with a relatively coarse model. The more refined the model, the more accurate the solution. The axisymmetric nature of the stand pipe led to the development of two quarter models as shown in Figures 5 and 6.

The most important ingredients needed to obtain accurate analytical results involved the determination of the material properties and a reasonable estimate of the wall thickness of the elements in the weld region. The thickness data was obtained by measuring several sliced sections from a typical pipe weld. An estimate of the material properties across the weld was obtained from some special reports supplied by our metallurgist.

Both of the resulting models allowed one to vary the thickness and material properties as a function of the axial direction, Z or X_i. (See

Appendix B for more model details.) In both models the following assumptions were made:

1. The loads (thermal deformations) are axisymmetric with respect to the X_i axis.

2. The material properties vary along the weld region in the X_i direction but are constant in the circumferential (hoop) direction.

3. Hookes law is obeyed.

Model "a" consists of two straight sections of pipe, one 304 stainless steel, the other carbon steel. This situation, which is very similar to the second classical analysis (Case B), resulted in thermally induced stress levels below the yield point of the materials.

Model "b" is very similar to Model "a" but in this case the boundary conditions in the tapered section of the carbon steel were modified to simulate the rigidity of the flange. This model very closely simulates the real boundary conditions. The stress levels were somewhat higher than those determined from Model "a," but still below yield. Close inspection of the weld region indicated that a much more refined model would be required to determine the peak stress levels at the beginning of the weld near the heat affected zone. A plot showing the thermally deformed weld region is presented in Figure 7.

To compensate for the relatively coarse grid network used in Models "a" and "b", a suitable stress concentration factor was determined. Application of this stress amplication factor indicated that the peak stress levels in the region of the failure would be between 137.9 MPa and 172.37 MPa (20,000 to 25,000 psi) depending on the quality (roughness) of the weld.

These results definitely showed that one must reasonably account for material property variation across a weld joining two different materials if there is to be any hope of obtaining a reasonable answer. However, these stress levels, which agreed with the deformation patterns determined from visual inspection of two failed pipes, left me with another dilemma. At these stress levels and only a few load cycles, failure should not occur. In addition, the ductility should not have decreased substantially. This region would have had to be precracked during fabrication or there was something yet to be uncovered.

At this point, I talked with some of the maintenance personnel who were performing the field welding. They stated that occasionally when they tried to reweld the cracked region after proper grinding of the crack, the material would essentially crumble when they began welding. The material was seemingly very brittle, i.e., had lost its ductility. This was further evidence that some additional mechanism was contributing to the failures.

Fortunately, by this time the TEC Materials Laboratory was able to mount samples of a typical failure and obtain metallographic* photos. From these photos, the reason for the failures became obvious. It was stress-corrosion-cracking, SCC[3,4,5,6], as is evident in Figure 8. By this time failures of 304 S.S. bourdon tubes and stainless steel rupture disks were also being encountered. Typical metallographic photos of these failures are shown in Figures 9 and 10. Thus, the puzzle began to fit together. We had determined that relatively high stress levels existed in the weld region. We were also aware that relatively large residual stresses could be present in the heat affected zone below the weld. Such stress levels in the presence of the proper chemical would readily explain the fill pipe failures. Usually, chlorides are the chief suspect for SCC in 300 series stainless steels, but no chloride source was immediately obvious. Thus we had to establish that chlorides were at fault and not some other chemical, then determine the source of the chlorides or other chemical.

This led to a review of the procedure for manufacturing the spin blocks, the cleaning procedure and chemicals used for cleaning, and a check of the chloride concentration in the heat-transfer fluid being used in the spin block.

This review was essentially fruitless. There was nothing that obviously stood out as a source of the chlorides. The chloride level in the heat-transfer fluid was found to be between 2 and 3 ppm. This concentration level was not nearly sufficient to cause the SCC being encountered.

Again, we had a dilemma. At this time we contacted the Kodak Materials Laboratory at Kodak Park, Rochester, New York. Discussions with Kodak Material's engineers revealed that they had encountered corrosion problems in a closed system where too much moisture (H_2O) was present. They had found that the moisture would move to the coolest part of the system where condensation and revaporization would occur repeatedly. In our system such an internal reflux condition would serve to leach chlorides from the heat-transfer fluid and concentrate them in the revaporization zone.

Subsequent infra-red temperature measurements substantiated the reflux theory. As shown in Figure 11, the temperatures in the upper carbon steel portion of the fill pipes that had previously failed were quite cool in relation to the heat-transfer fluid temperature. Thus, the failures in this relatively high temperature environment were attributed to stress-corrosion-cracking which was a result of:

1. The welding of two materials with different coefficients of thermal expansion;

2. The high operating temperature and the associated stress fields; and

3. The presence of a mechanism to concentrate chlorides, i.e., a water/steam reflux cycle.

*A standard polishing procedure with an acid etch was employed.

The fill pipes that had not failed, did not show a temperature change in the weld to flange region. This indicated that these units did not contain sufficient moisture to establish the required water/steam reflux system for concentrating chlorides.

From these results it was concluded that the problem could be corrected by either changing the flange material or by removing the moisture from the system. The latter corrective action was taken.

Thus, through the cooperation and assistance from maintenance personnel (welders), production personnel, and material engineers at TEC and Kodak, I was finally able to establish the complete mechanism that was causing the failures. Such, interdisciplinary interactions are often a necessity in solving such unusual problems.

CONCLUSION

This analysis clearly shows the merits of the finite element method as available in NASTRAN. This capability allows the engineer to much more closely simulate real life situations and thus obtain more reasonable/accurate results. This is particularly helpful in failure analysis since conservative results do little more than cover up the real cause of a failure. Only in the design process should one consider conservative methods. But even in this case, one must be very cautious.

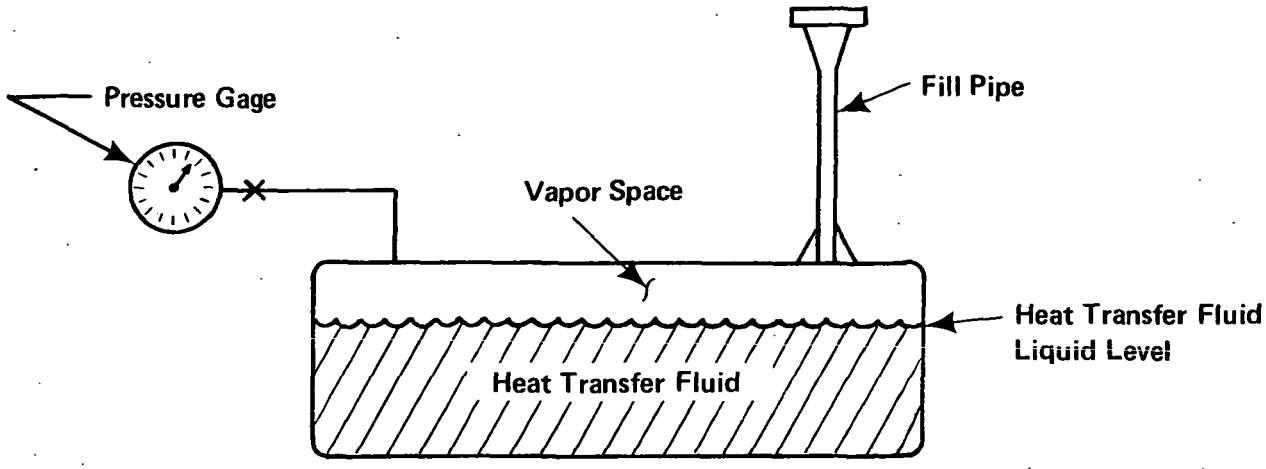

Figure 1: SPIN Block Schematic

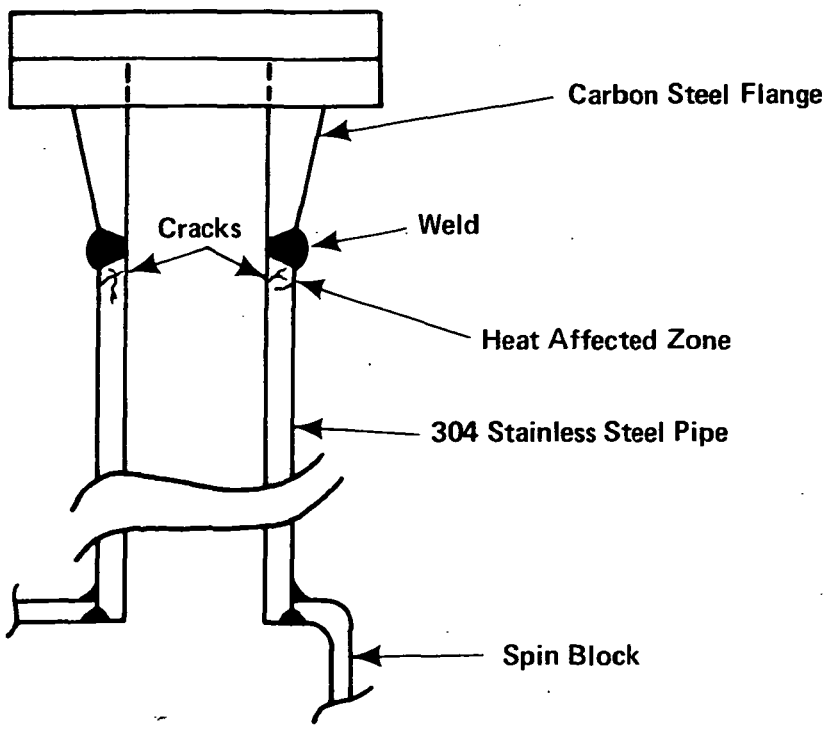

Figure 2: Fill Pipe Detail

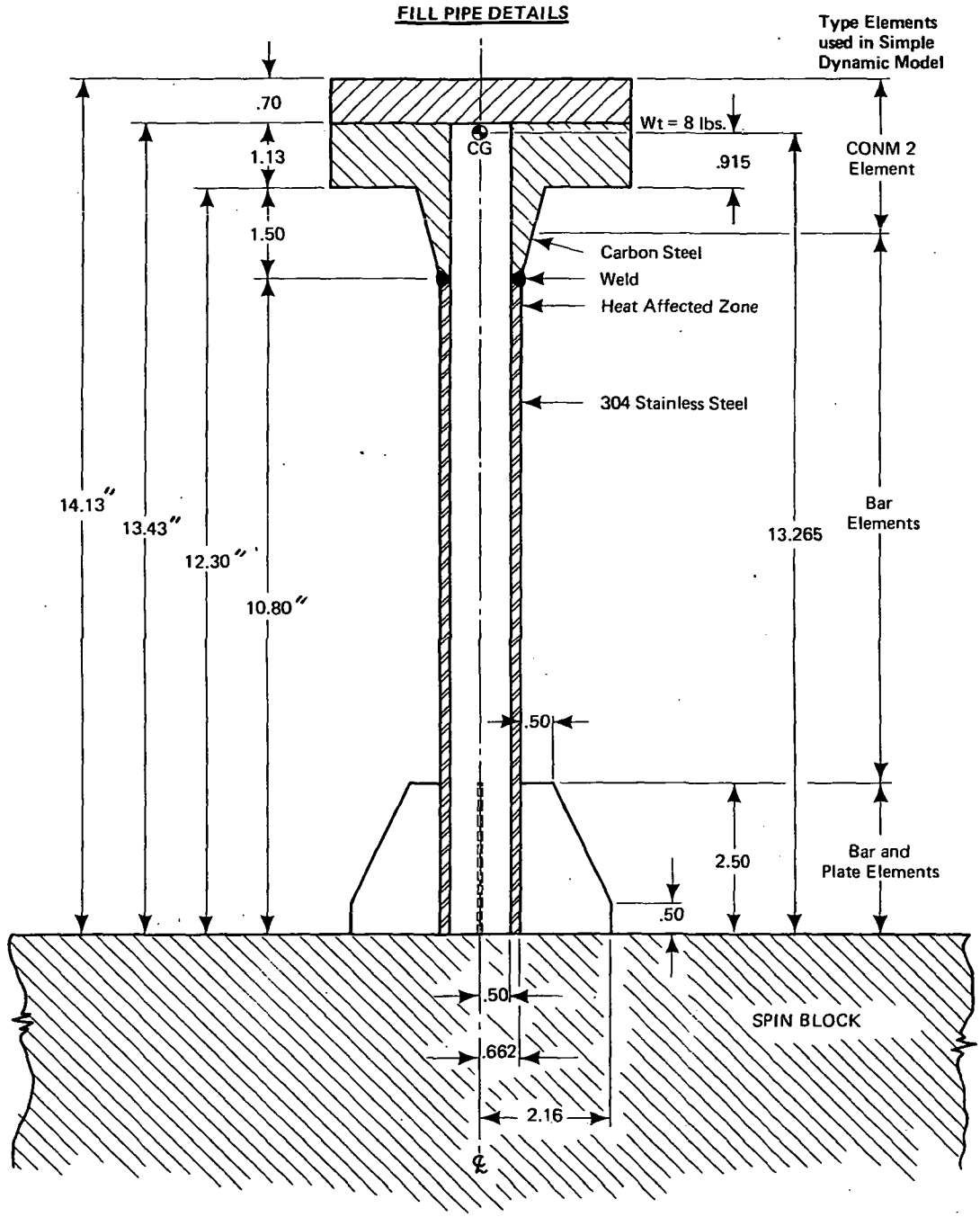

Figure 3: Fill Pipe Schematic Drawing

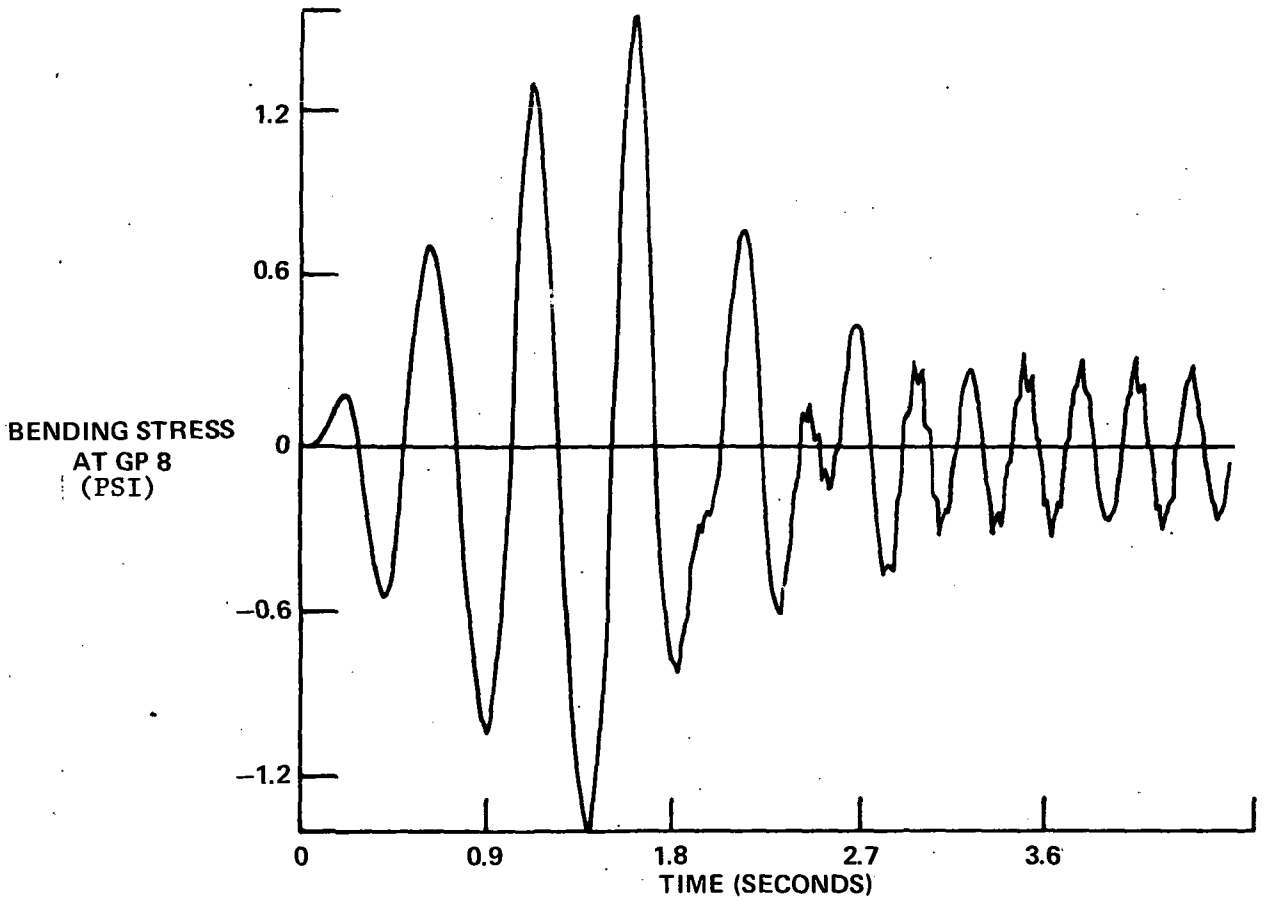

Figure 4: Bending Stress vs Time (Force Response Analysis)

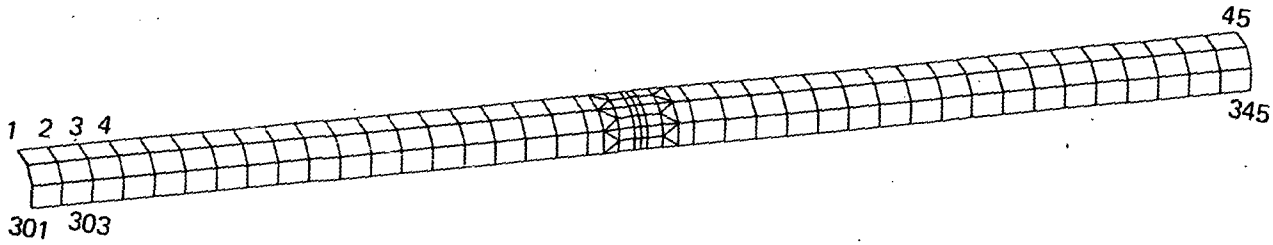

Figure 5: NASTRAN Model a

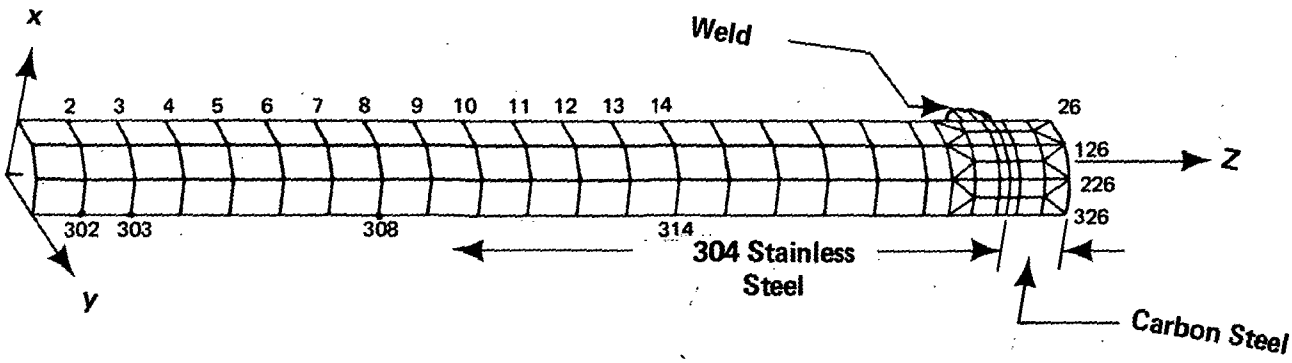

Figure 6: NASTRAN Model b

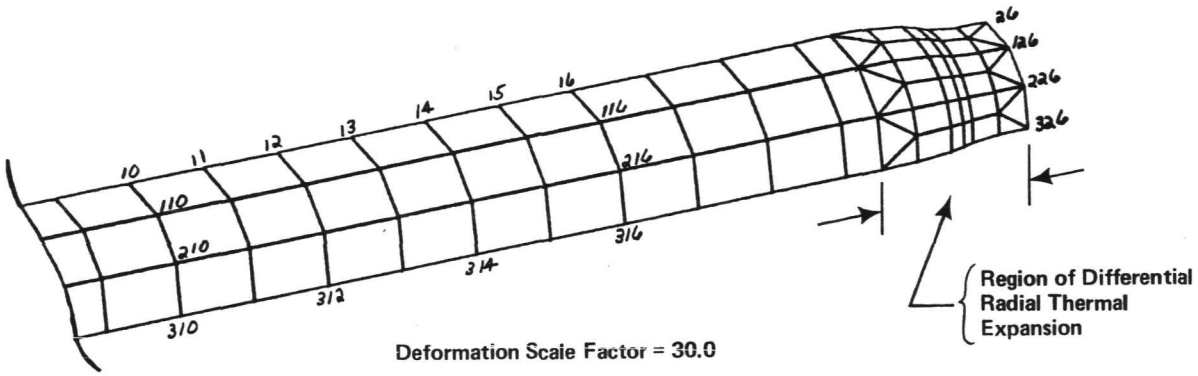

Figure 7: NASTRAN Deformed Plot of Model b

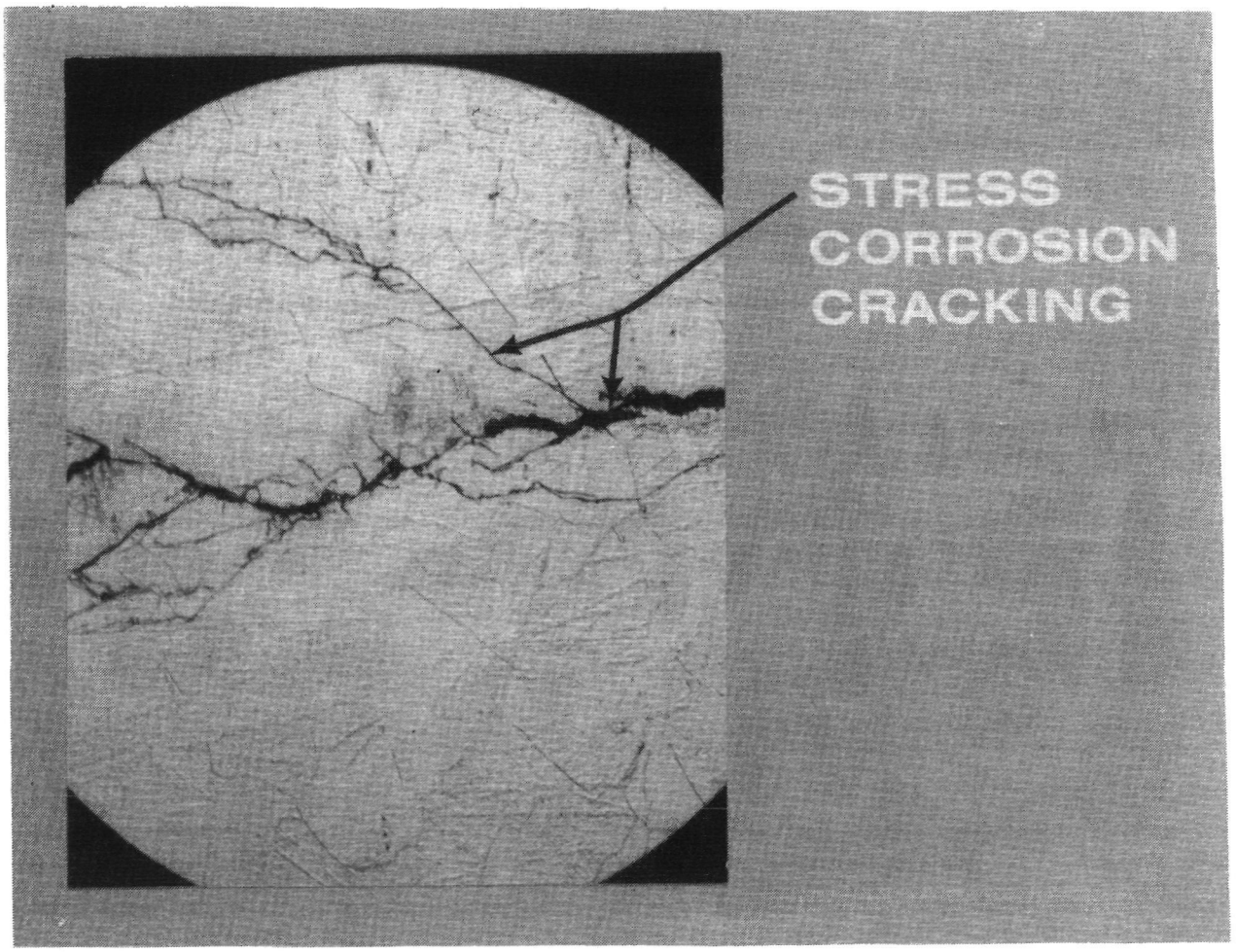

Figure 8: Photomicrograph Showing Stress Corrosion Cracking in the 304 Stainless Steel Transition Region of the Fill Pipe

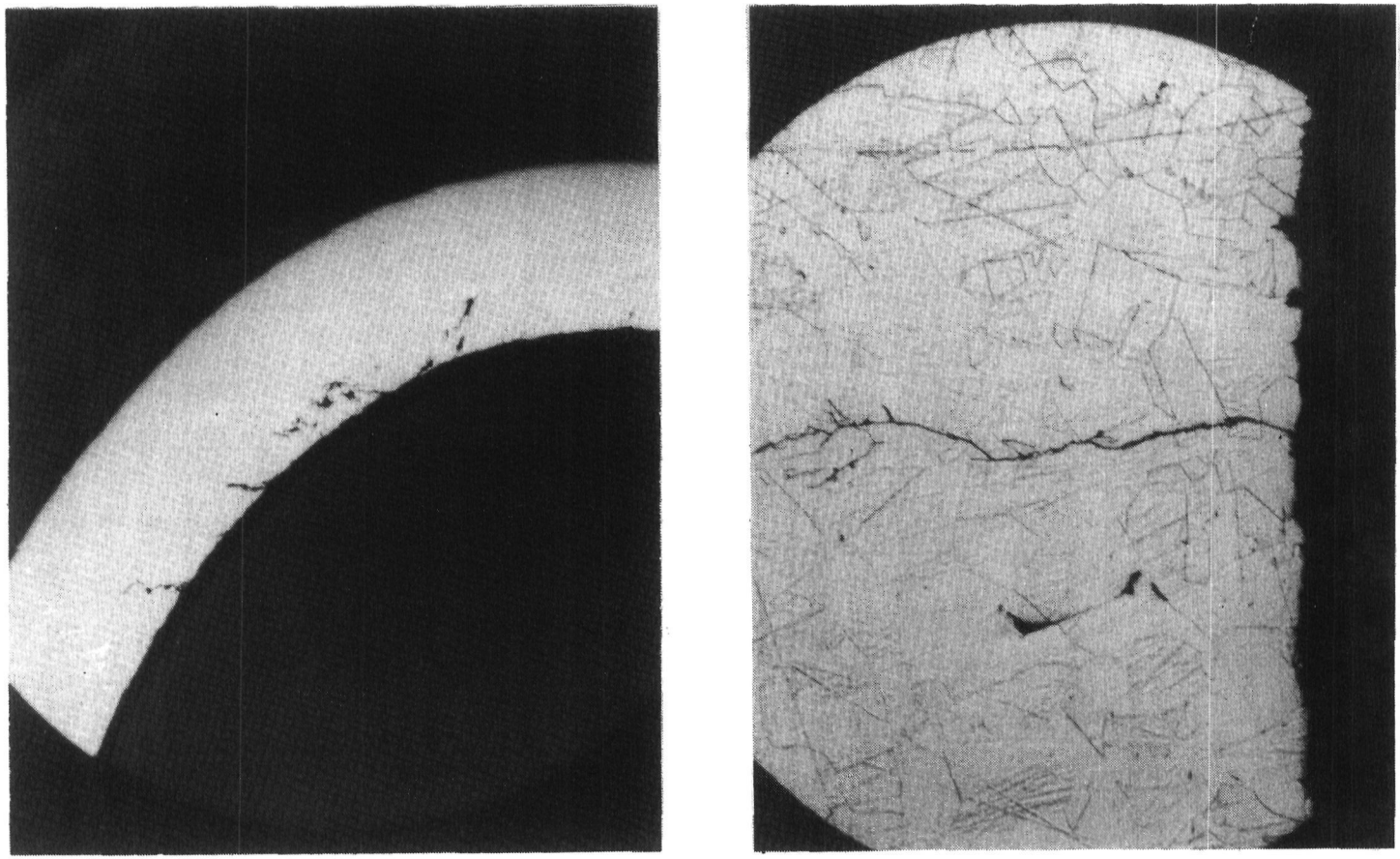

Figure 9: Photomicrographs Showing Stress Corrosion Cracking in a 304 Stainless Steel Bourdon Tube

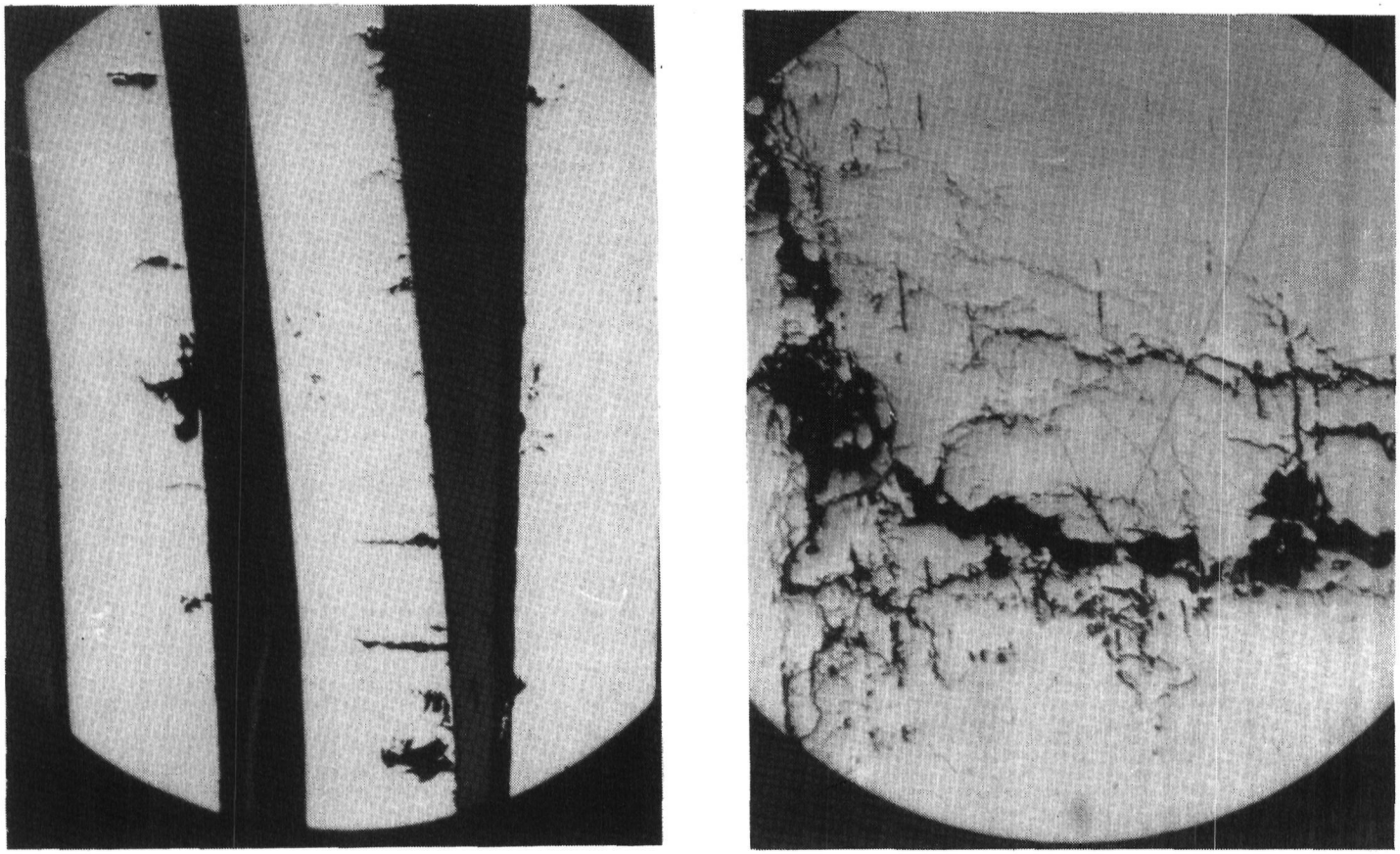

Figure 10: Additional Photomicrographs Showing Stress Corrosion Cracking in Other Fill Pipes and in the 304 Stainless Steel Pressure Relief Piping System

Temperature (°F)					
Spin Block No.	T_1	T_2	T_3	T_4	T_5
2-7	300	200	<200	<200	<200
2-8	290	200	<200	<200	<200
2-9	470	475	475	320	200
3-8	–	200	<200	<200	<200

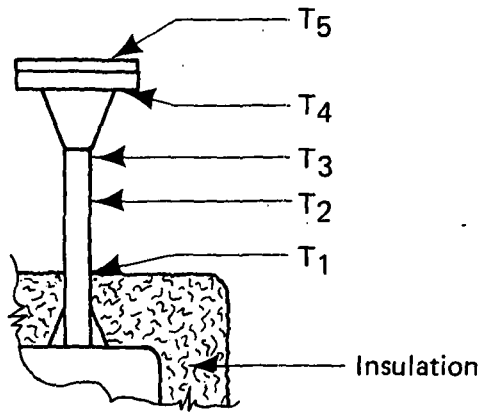

Figure 11: Thermal Profiles of Fill Pipes That Had Previously Failed

APPENDIX A

Nomenclature: (See References 1 and 2.)

P_i = Shear load (lbf)
M_i = Moment (in-lbs)
E_i = Modulus of Elasticity (psi)
υ = Poisson's Ration
r_i = Outside Radius of Pipe (inches)
t_i = Wall Thickness (inches)
T = Temperature (°F)
Θ_i = Slope
y_i = Deflection (inches)
$I_i = bt^3/12 = t^3/12$

Case A: Conservative Case
Stainless Steel Pipe to a Rigid Carbon Steel Block

Assumption: Stainless steel pipe is infinitely long, thus semi-infinite beam on elastic foundation theory is applicable.

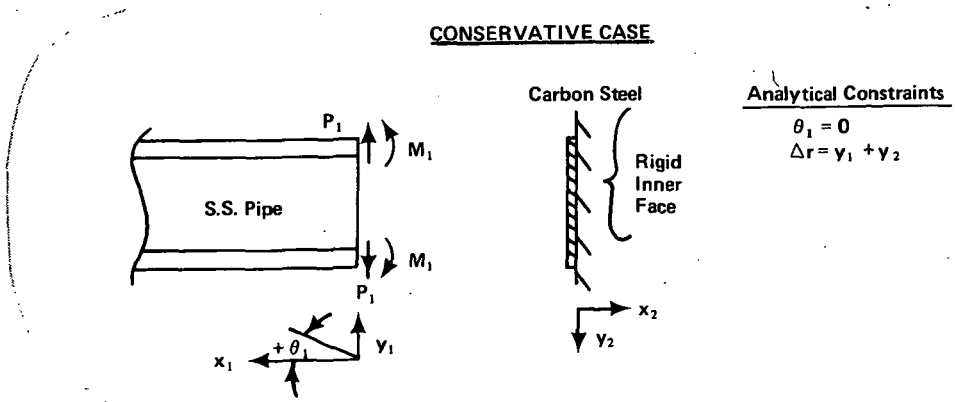

Analytical Conditions and Data

$y \neq 0$
$\Theta_1 = 0$
$T = 536°F = T_1 = T_2$
$T_0 = 72°F$
$\alpha_1 = 9.76 \times 10^{-6}$ in/in/°F
$\alpha_2 = 7.12 \times 10^{-6}$ in/in/°F
$r_1 = .73"$
$t_1 = .137"$

Differential Radial Expansion

$$\Delta r = (r_1\alpha_1 - r_2\alpha_2)(T - T_0)$$

Applicable Equations

$$y_1 = \left[P_1/2E_1I_1\beta_1^3 \right] D_{\beta x} - \left[M_1/2E_1I_1\beta_1^2 \right] C_{\beta x}$$

$$\theta_1 = -\left[P_1/2E_1I_1\beta_1^2 \right] A_{\beta x} + \left[M_1/\beta_1 E_1 I_1 \right] D_{\beta x}$$

Final Equations

(1) $y_1 = \Delta r$

which leads to

$$-.175P_1 + .716M_1 = -14,400$$

(2) $\theta_1 = 0$

which leads to

$$P = 2\beta_1 M_1 = 8.18M_1$$

Case B: Non-Conservative Case

Carbon Steel - Stainless Steel Pipe Junction

Assumption: Both pipes are infinitely long, i.e., semi-infinite beams on an elastic foundation.

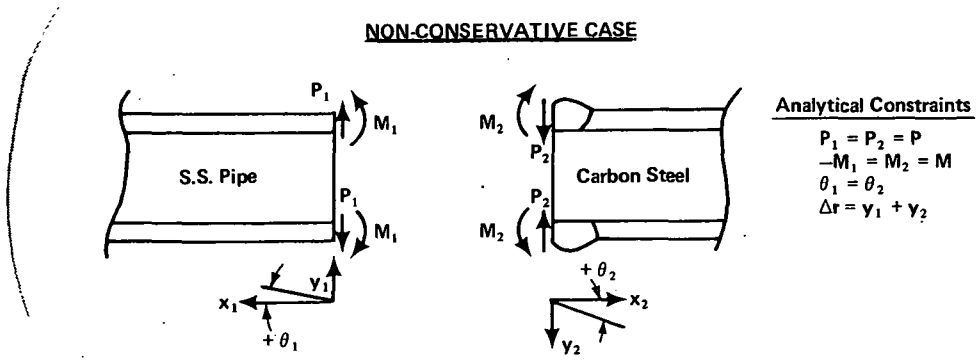

Analytical Conditions and Data

$-M_1 = M_2 = M$
$P_1 = P_2 = P$
$\Theta_1 = \Theta_2$
$\Delta r = y_1 + y_2$
$T = 536°F = T_1 = T_2$
$\Delta T_1 = \Delta T_2$

$\alpha_1 = 9.76 \times 10^{-6}$ in/in/°F
$\alpha_2 = 7.12 \times 10^{-6}$ in/in/°F
$r_1 = .73"$
$r_2 = .783"$
$t_1 = .135"$
$t_2 = .240"$

Differential Radial Expansion

$$\Delta r = r_1 d_1 (\Delta T_1) - r_2 \alpha_2 \Delta T_2 = y_1 + y_2$$
$$\Delta r = \Delta T(r_1 d_1 - r_2 d_2)(T - T_0)$$

Applicable Equations

$$y_i = \left[P_i / 2E_i I_i \beta_i^3\right] D_{\beta x} - \left[M_i / 2E_i I_i \beta_i^2\right] C_{\beta x}$$
$$\Theta_i = -\left[P_i / 2E_i I_i \beta_i^2\right] A_{\beta x} + \left[M_i / \beta_i E_i I_i\right] D_{\beta x}$$

$$\beta_i = \sqrt[4]{3(1 - \upsilon^2)/r^2 t^2}$$

$$\begin{aligned} A_{\beta x} &= e^{-\beta x}\,[\cos(\beta x) + \sin(\beta x)] \\ B_{\beta x} &= e^{-\beta x}\,[\sin(\beta x)] \\ C_{\beta x} &= e^{-\beta x}\,[\cos(\beta x) - \sin(\beta x)] \\ D_{\beta x} &= e^{-\beta x}\,[\cos(\beta x)] \end{aligned}$$

Final Equations

(1) $\Delta r = y_1 + y_2$

which leads to

$.5424P - .373M = 7200$

(2) $\Theta_1 = \Theta_2$ or $\Theta_1 - \Theta_2 = 0$

which leads to

$P = 33.04M$

APPENDIX B

Additional NASTRAN Model Details

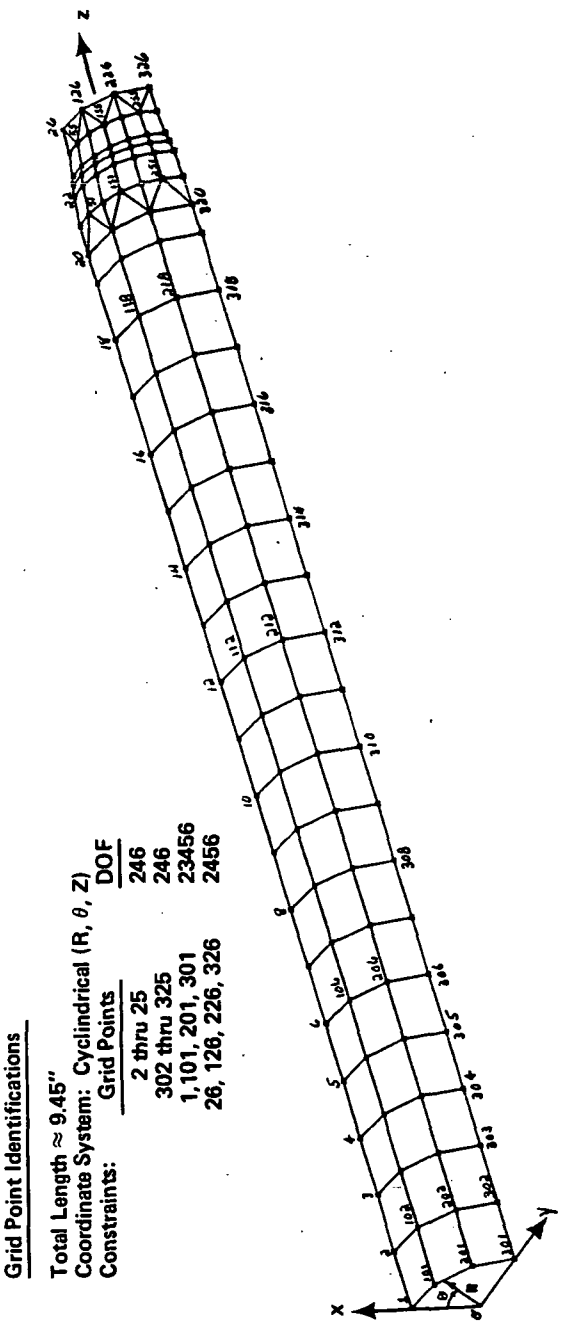

Grid Point Identifications

Total Length ≈ 9.45"
Coordinate System: Cylindrical (R, θ, Z)
Constraints:

Grid Points	DOF
2 thru 25	246
302 thru 325	246
1, 101, 201, 301	23456
26, 126, 226, 326	2456

Element Identification

Type Elements: CQUAD2, CTRIA2
Load: Temperature at 536°F
Thermal Coef. of Expansion:
α S.S. = 9.76 x 10^{-6} in/in/°F
α C.S. = 7.12 x 10^{-6} in/in/°F

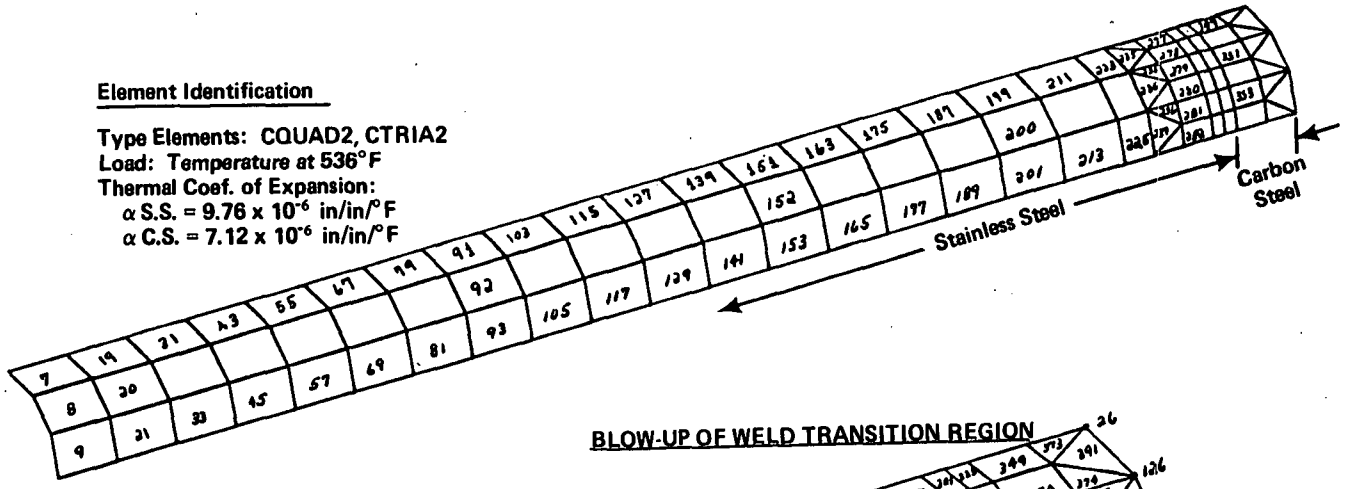

BLOW-UP OF WELD TRANSITION REGION

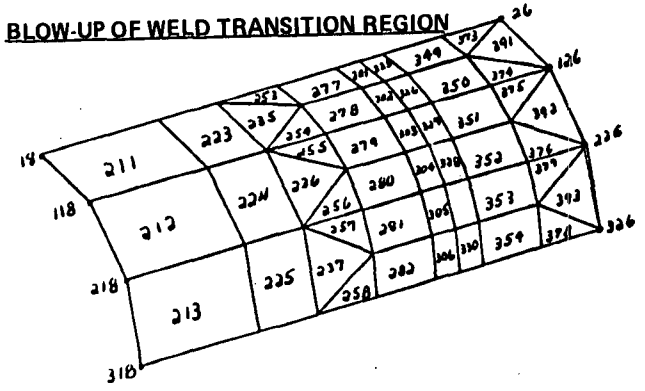

REFERENCES

1. Theory and Design of Modern Pressure Vessels, 2nd Edition, by John F. Harvey, pp. 134-166, especially Section 4.8.

2. Beams on Elastic Foundations, by M. Hetenyi, pp. 30-37.

3. Stress Corrosion Cracking in High Strength Steels and in Titanium and Aluminum Alloys, edited by B. F. Brown, Naval Research Laboratory. (U.S. Government Printing Office, Stock No. 0851-0058).

4. Stress Corrosion Cracking Control Measures, National Bureau of Standards, Monograph 156, B. F. Brown, 1977.

5. Success by Design; Progress Through Failure Analysis, National Bureau of Standards (NBS), Publication 433, MPFG 25th Meeting, edited by T. R. Shives and W. A. Willard, 1974.

6. Engineering Design, MFPG 25th Meeting, National Bureau of Standards, Special Publication 487, 1977.

7. Mechanical Failure; Definition of the Problem, MFPG 20th Meeting, National Bureau of Standards Special Publication 423, 1976.

8. NASTRAN User's Manual, NASA SP-222(05), Available from COSMIC, University of Georgia.